Available online at www.sciencedirect.com
SCIENCE DIRECT®
Biochemical Pharmacology 68 (2004) 1889–1902
Biochemical Pharmacology
www.elsevier.com/locate/biochempharm

In vitro metabolism of cyclosporine A by human kidney CYP3A5

Yang Dai[a], Kazunori Iwanaga[a,b], Yvonne S. Lin[a,c], Mary F. Hebert[d], Connie L. Davis[e], Weili Huang[a], Evan D. Kharasch[f], Kenneth E. Thummel[a,*]

[a]*Department of Pharmaceutics, University of Washington, Seattle, WA 98195, USA*
[b]*Osaka University of Pharmaceutical Sciences, Osaka, Japan*
[c]*St. Jude Children's Research Hospital, Memphis, TN, USA*
[d]*Department of Pharmacy, University of Washington, Seattle, WA 98195, USA*
[e]*Department of Medicine, Division of Nephrology, University of Washington, Seattle, WA 98195, USA*
[f]*Department of Anesthesiology, University of Washington, Seattle, WA 98195, USA*

Received 6 May 2004; accepted 12 July 2004

Abstract

The objectives of this study were to characterize and compare the metabolic profile of cyclosporine A (CsA) catalyzed by CYP3A4, CYP3A5 and human kidney and liver microsomes, and to evaluate the impact of the CYP3A5 polymorphism on product formation from parent drug and its primary metabolites. Three primary CsA metabolites (AM1, AM9 and AM4N) were produced by heterologously expressed CYP3A4. In contrast, only AM9 was formed by CYP3A5. Substrate inhibition was observed for the formation of AM1 and AM9 by CYP3A4, and for the formation of AM9 by CYP3A5. Microsomes isolated from human kidney produced only AM9 and the rate of product formation (2 and 20 μM CsA) was positively associated with the detection of CYP3A5 protein and presence of the *CYP3A5*1* allele in 4 of the 20 kidneys tested. A kinetic experiment with the most active *CYP3A5*1*-positive renal microsomal preparation yielded an apparent K_m (15.5 μM) similar to that of CYP3A5 (11.3 μM). Ketoconazole (200 nM) inhibited renal AM9 formation by 22–55% over a CsA concentration range of 2–45 μM. Using liver microsomes paired with similar CYP3A4 content and different CYP3A5 genotypes, the formation of AM9 was two-fold higher in *CYP3A5*1/*3* livers, compared to *CYP3A5*3/*3* livers. AM19 and AM1c9, two of the major secondary metabolites of CsA, were produced by CsA, AM1 and AM1c when incubated with CYP3A4, CYP3A5, kidney microsomes from *CYP3A5*1/*3* donors and all liver microsomes. Also, the formation of AM19 and AM1c9 was higher from incubations with liver and kidney microsomes with a *CYP3A5*1/*3* genotype, compared to those with a *CYP3A5*3/*3* genotype. Together, the data demonstrate that CYP3A5 may contribute to the formation of primary and secondary metabolites of CsA, particularly in kidneys carrying the wild-type *CYP3A5*1* allele.

Keywords: Cyclosporine A; CYP3A5; Genetic polymorphism; Drug metabolism; Nephrotoxicity

1. Introduction

Renal dysfunction caused by the use of calcineurin inhibitor (e.g., cyclosporine and tacrolimus)—based immunosuppression therapy is a common long-term complication of organ transplantation [1]. For example, in a recent retrospective study of patients who had undergone liver transplantation, we found that approximately one-third of those who received cyclosporine A (CsA) as part of their postoperative immunosuppression therapy had markedly elevated serum creatinine (SCr >1.6 mg/dl) 3 years post-transplantation [2]. In another study by Fisher et al. [3], the authors reported that 80% of liver transplant patients receiving CsA and surviving 5 years or more had elevated SCr (>1.4 mg/dl). Moreover, the cumulative incidence of end-stage renal disease (ESRD) requiring hemodialysis or kidney transplantation is about 3–10% in long-term survival patients and increases with survival time [3–6]. The use of CsA as part of immunosuppression therapy is believed to be a major cause of chronic renal dysfunction and renal failure. CsA alters the proper

Abbreviations: CsA, Cyclosporine A; C_{trough}, trough blood concentration; $C_{2\ hour}$, two-hour blood concentration; AUC, area under the curve

* Corresponding author. Tel.: +1 206 543 0819; fax: +1 206 543 3204.
E-mail address: thummel@u.washington.edu (K.E. Thummel).

0006-2952/$ – see front matter © 2004 Elsevier Inc. All rights reserved.
doi:10.1016/j.bcp.2004.07.012

function of cultured renal tubular epithelial and mesangial cells [7–9]. In addition, it is associated with damage to renal tubular epithelium, mesangium and afferent glomerular arterioles in vivo [10], and the accumulation of collagen and other matrix proteins produced by tubular cells in the renal interstitium [11]. These findings suggest that accumulation of CsA or its metabolites within renal cells may be a critical determinant of renal dysfunction.

Close therapeutic monitoring of unchanged CsA concentration in blood (C_{trough}, $C_{2\ hour}$ or AUC monitoring) has been adopted to reduce the incidence of graft rejection and CsA toxicity. However, CsA blood concentration and dose were found not to be strongly associated with the occurrence of renal dysfunction [3,12,13]. Thus, it has been suggested that inter-individual differences in the systemic profile of cyclosporine metabolites and renal disposition of CsA and its metabolites contribute to the divergent adverse drug response to a therapeutic systemic CsA exposure level [14].

CsA undergoes extensive biotransformation to more than 30 metabolites [15]. Among these, the primary metabolites AM1, AM9 and AM4N, and some secondary and tertiary metabolites, AM1c, AM19 and AM1c9, are abundant in the blood, urine and bile [16–18]. These major CsA metabolites are the product of cytochrome P4503A (CYP3A) catalytic activity [19,20]. CsA and its metabolites are also substrates for P-glycoprotein (P-gp), a major xenobiotic efflux pump in humans [21–23]. Both CYP3A and P-gp are found in the liver, intestine and kidney. Hepatic CYP3A and intestinal P-gp contribute to the low systemic bioavailability (20–30%) of CsA after oral administration [24]. CYP3A and P-gp in the liver are also responsible for the systemic clearance of CsA from blood [25]. Hepatic P-gp may also play a major role in the biliary excretion of CsA metabolites [26]. Thus, inter-individual variability in the systemic blood concentration of CsA and its metabolites might be explained by differences in the expression and function of CYP3A and P-gp in the liver and intestine.

The primary metabolites of CsA are reportedly much less toxic to cultured renal cells than parent drug [7,27,28]. Consequently, the metabolism of CsA to its primary metabolites may represent a detoxification pathway. Indeed, some investigators report a positive association between low hepatic CYP3A content or activity and increased incidence of CsA renal toxicity after liver transplantation [29,30]. In contrast, Christians et al. [31] found an inverse correlation between the steady-state blood concentration of AM1c9, a secondary CsA metabolite, and renal function in liver transplant patients during the early post-operative period. Yet another group [32] found elevated urine AM19 levels in patients with histologically confirmed CsA nephrotoxicity late after renal transplantation. However, elevated CsA metabolites in patients with impaired renal function could be the result, rather than the cause, of CsA nephrotoxicity. Or, alternatively, individual variability in the formation and accumulation of CsA metabolites in blood could contribute directly to differences in renal toxicity risk. In this regard, formation of AM1c9 and AM19 may represent a toxification pathway. Thus, elucidation of the metabolic profile of CsA for individual patients may be key to understanding individual risk of nephrotoxicity.

Although CYP3A4 and CYP3A5 are the dominant CYP3A isoforms found in adult human tissues, only CYP3A5 is expressed to any significant degree in renal tubular epithelial cells [33–35]. CYP3A5 is a polymorphic enzyme. A splicing variant, *CYP3A5*3*, has been identified as the major cause of variable expression of CYP3A5 in the liver and intestine [36–38]. In the kidney, this mutation also results in polymorphic CYP3A5 expression and midazolam hydroxylation activity [35]. Kidney microsomes from *CYP3A5*1/*3* individuals exhibited an eight-fold higher mean microsomal CYP3A5 content and 18-fold higher midazolam hydroxylation activity than those of *CYP3A5*3/*3* individuals. With respect to CsA metabolism, Aoyama et al. [20] found that the two CYP3A isoforms exhibit different product regioselectivity. Three major metabolites (AM1, AM9 and AM4N) are formed by CYP3A4. In contrast, only AM9 is formed by CYP3A5.

Based on this information, we hypothesized that the *CYP3A5* genetic polymorphism may influence the metabolism of CsA and production of its primary and secondary metabolites in the liver and renal tubular epithelial cells, resulting in different systemic and intra-renal drug/metabolite exposures and differential risk of nephrotoxicity. The purpose of the present study was to confirm the in vitro metabolic profile of CsA and its metabolites using heterologously expressed CYP3A4 and CYP3A5 and to determine the effect of *CYP3A5* genotypes on the metabolic fate of CsA following incubation with kidney and liver microsomes.

2. Materials and methods

2.1. Materials

Cyclosporine A, testosterone, and NADPH were obtained from Sigma Chemical Company (St. Louis, MO). Ketoconazole was acquired from Research Diagnostics, Inc. (Flanders, NJ). Cyclosporine metabolites, AM1, AM1c, AM9 and AM4N, were kindly provided by Dr. Paul B. Watkins, University of North Carolina-Chapel Hill. 6β-Hydroxytestosterone and 11α-progesterone were obtained from Steraloids (Newport, RI). Methanol, acetonitrile and ethyl acetate were purchased from Fisher Scientific (Santa Clara, CA). Heterologous baculovirus-insect cell expressed human CYP3A4 SUPERSOMES™ (Catalog No. 456207/P207), human CYP3A4 + b_5 SUPERSOMES™ (Catalog No. 456202/P202) and human CYP3A5

SUPERSOMES™ (Catalog No. 456235/P235) were purchased from BD Gentest (Woburn, MA). Cytochrome b_5 was purchased from PanVera (Carlsbad, CA).

2.2. Tissue samples

The collection and use of human tissue for research was approved by the University of Washington Human Subjects Review Board. Samples of 60 human livers from Caucasian donors were obtained from the University of Washington School of Pharmacy Human Tissue Bank (Seattle, WA). Human liver microsomes were prepared according to previously published protocols [39].

Twenty adult human kidneys were obtained from the National Disease Research Interchange (Philadelphia, PA). Upon delivery to our lab, the kidneys were cut into ~5 g pieces and stored at −80 °C. Human kidney microsomes were prepared using a previously published method [39], with some modifications. Briefly, a complete protease inhibitor cocktail tablet (1 tablet/50 ml, Roche Applied Science, Indianapolis, IN) was dissolved in homogenizing buffer (10 mM potassium phosphate, 0.25 M sucrose and 1 mM EDTA, pH 7.4) immediately before use. Cold homogenization buffer was then added to ~15 g of frozen kidney tissue. When slightly thawed, the tissue was cut into smaller pieces with scissors and was blended for 15 s (10 s on low and 5 s on high speed). More homogenization buffer was added for a final dilution of approximately four-fold (w/v). The mixture was transferred to a glass Thomas tube and homogenized using a motor-driven Telflon-tipped pestle (8–10 strokes) while on ice. The homogenate was filtered through sterile gauze, transferred to 30-ml tubes and centrifuged at 11,000 × *g* for 30 min. The resulting supernatant was transferred to clean tubes for high-speed centrifugation at 110,000 × *g* for 70 min. The resulting pellet was resuspended in wash buffer (10 mM potassium phosphate, 0.15 mM potassium chloride and 1 mM EDTA, pH 7.4), transferred to a Thomas tube for resuspension of the microsomes (8–10 strokes) and centrifuged again at 110,000 × *g* for 70 min. The washed pellet was resuspended in 10 ml storage buffer (0.25 M sucrose and 1 mM EDTA, pH 7.4), and aliquots of the final microsomal suspension (~0.3 ml) were stored at −80 °C. Protein concentrations were determined by the method of Lowry [40], using bovine serum albumin as the reference standard.

2.3. Western blot analysis

CYP3A4 (purified from human liver) and CYP3A5 (purified from a heterologous baculovirus-insect cell expression system) were used as reference standards (specific contents were 12.2 and 11.7 nmol P450/mg protein). Total protein concentration for the CYP3A standards was determined by the method of Lowry, using bovine serum albumin as a reference protein. Total P450 content was determined from the CO binding spectra [41].

Immunoquantitation of CYP3A4 and CYP3A5 was performed as described by Paine et al. [39], with minor modifications. Briefly, kidney microsomal protein (3 μg for kidneys expressing one *CYP3A5*1* allele and 20 μg for *CYP3A5*3/*3* kidneys) was resolved by electrophoresis on 9% acrylamide gels. To control for matrix effects, kidney microsomes with nearly undetectable CYP3A4 or CYP3A5 levels were added to CYP3A4 or CYP3A5 standard curves. The amount of protein added to CYP3A4 or CYP3A5 standard curves was equivalent to that of the kidney samples being analyzed. Following electrophoresis, the gels were cut using molecular weight standards as markers, and the resulting strips were placed on sheets of nitrocellulose for simultaneous electrophoretic transfer. The nitrocellulose sheets were incubated with a specific anti-CYP3A5 IgG antibody (Gentest, Woburn, MA) or an anti-CYP3A4 antibody [42]. Although the anti-CYP3A4 antibody cross-reacts with CYP3A5, the SDS–PAGE conditions used in this experiment resulted in physical separation of CYP3A4 and CYP3A5 bands, and thus should give a reliable quantification of CYP3A4 content. CYP3A5 content was determined using the specific anti-CYP3A5 antibody. An Integrated Optical Density (IOD) for each BCIP-NBT developed protein band was generated using a Bio-Rad ChemiDoc and Quantity One program (Hercules, CA). CYP3A protein levels in the tissue preparations were estimated by comparison of the unknown band IOD to the appropriate standard curve.

2.4. Kidney microsomal testosterone 6β-hydroxylation

Testosterone, an excellent substrate (6β-hydroxylation) for both CYP3A4 and CYP3A5 [43], was used to characterize the CYP3A activity of kidney microsomal preparations. Kidney microsomes (0.4 mg/ml in KPi, pH 7.4) were incubated with 200 μM testosterone and 1 mM NADPH in 1 ml incubation volume for 15 min. The reactions were terminated by addition of 5 ml ethyl acetate. After adding 50 ng internal standard (11α-progesterone) and brief mixing, the organic layer was removed and evaporated under a gentle nitrogen stream. Testosterone, 6β-hydroxytestosterone and 11α-progesterone concentrations were measured by HPLC, as modified from the method of Fisher et al. [44]. Briefly, the solid extract was reconstituted in 100 μl of methanol/H_2O (1:1, v/v) and 20 μl was injected onto an Agilent 1100/1050 Series HPLC (Agilent Technologies, Wilmington, DE) equipped with a Develosil ODS-UG-5 column (4.6 mm × 100 mm, 5 μm) obtained from Phenomenex (Torrance, CA). Testosterone and 6β-hydroxytestosterone were detected at 240 nm and peak areas were converted to concentrations by comparison with peaks from the standard samples over a concentration range of 31–1000 ng/ml. The retention time for 6β-hydroxytestosterone, 11α-progesterone and testosterone were 3.4, 8.3 and 10.2 min, respectively.

2.5. Cyclosporine A kinetic protocols

All incubations were performed in duplicate in solutions containing 0.1 M potassium phosphate, pH 7.4, and 1 mM EDTA. The final incubation volume was 0.5 ml. The incubation temperature was 37 °C. Cyclosporine A and ketoconazole were dissolved in methanol and added into the incubation solutions to the desired concentrations. The final methanol concentration was less than 4%. Conditions that conferred linear product formation with respect to time and protein were determined.

CYP3A4, CYP3A4 + b_5 and CYP3A5 SUPERSOMES™ were employed for the estimation of kinetic parameters of CsA metabolite formation. CYP3A4 and CYP3A5 were supplemented with cytochrome b_5 (final molar concentration ratio in the incubation solution: cytochrome P450:cytochrome b_5 = 1:3). CsA (final concentration 0–256 μM) was added to the incubation tubes together with CYP3A4 (20 pmol/ml), CYP3A4 + b_5 (10 pmol/ml) or CYP3A5 (20 pmol/ml). The mixture was preincubated at 37 °C for 5 min before addition of NADPH (final concentration 1 mM) or buffer (as negative control) to initiate the reaction. Reactions were terminated after 10 min (for CYP3A4 + b_5) or 15 min (for CYP3A4 and CYP3A5) by the addition of 0.5 ml cold acetonitrile.

CsA concentrations of 2 and 20 μM were used for comparison and screening of the metabolic activity of *CYP3A5*1* positive and negative human kidney microsomes (4 with *CYP3A5*1/*3* genotypes and 4 with *CYP3A5*3/*3* genotypes). The genotype of the kidneys from which microsomes were isolated had been determined previously [35]. The substrate concentrations were approximately 0.1 and 2 times the K_m determined from experiments with heterologously expressed CYP3A5. For kinetic parameter estimation, the kidney microsomal preparation with the highest CYP3A5 activity (HK-114B) was incubated with CsA over a concentration range of 2–45 μM.

Co-incubation of kidney microsomes with CsA and ketoconazole was conducted to confirm the involvement of CYP3A5 in the formation of CsA metabolites. For the inhibition experiment, ketoconazole (200 nM) was added to the incubations together with CsA (2–45 μM) and kidney microsomes (HK-114B). At that concentration, ketoconazole was projected to potently and selectively inhibit CYP3A4/5 (K_i = 109 nM, [45]), with little effect on other known renal microsomal P450 (e.g., CYP2C) enzymes. The final protein concentration in the kidney incubation mixture was 0.4 mg/ml. NADPH (final concentration, 1 mM) was added after a 5-min preincubation period and the incubation lasted 40 min.

For the comparison of CsA metabolism in *CYP3A5*1* positive and negative human livers, microsomes from livers with *CYP3A5*1/*3* genotype were paired with those with a *CYP3A5*3/*3* genotype that had similar CYP3A4 immunocontent. A total of 20 different microsomal preparations (10 pairs) were studied and the CYP3A5 genotype for these livers had been determined previously [38]. CsA concentrations of 2 and 20 μM were used and the protein concentration was 0.2 mg/ml. NADPH (final concentration, 1 mM) was added after a 5 min preincubation period and the incubation time was 10 min (2 μM CsA) or 20 min (20 μM CsA).

To evaluate the generation of secondary metabolites of CsA, parent drug, AM1 and AM1c (20 μM) were all incubated with each of the following enzyme preparations: CYP3A4 (500 pmol/ml supplemented with 1500 pmol/ml cytochrome b_5), CYP3A5 (500 pmol/ml supplemented with 1500 pmol/ml cytochrome b_5), liver microsomes (0.2 mg/ml) and kidney microsomes (0.4 mg/ml). The reactions were initiated by addition of NADPH (final concentration, 2.5 mM for heterologously expressed enzymes and 1 mM for liver and kidney microsomes) or buffer after a 5-min preincubation period and were terminated after 2 h.

CsA metabolites generated from each of the experiments described above were extracted with 5 ml of ethyl acetate. The solutions were shaken vigorously for 15 min and followed by centrifugation at 1330 × *g* for 10 min. The organic solvent was removed and evaporated to dryness under a stream of nitrogen at 40 °C. The remaining residue was then reconstituted in 0.1 ml methanol and stored at −20 °C. Twenty microliters from each sample was injected onto the LC/MS–MS for analysis.

2.6. LC/MS–MS assay for primary cyclosporine A metabolites

The quantification of cyclosporine A metabolites was accomplished using a liquid chromatography/tandem mass spectrometric (LC/MS–MS) assay adapted from the procedure of Simpson et al. [46]. Liquid chromatography was performed on a Shimadzu LC-10AD solvent delivery system equipped with a Shimadzu SIL-10ADVP autoinjector (Schimadzu Scientific Instruments, Inc., Columbia, MD) fitted with a Luna Phenyl-hexyl, 150 mm × 4.6 mm, 3 μm column and a SecurityGuard column (Phenomenex, Torrance, CA). The columns were heated to 70 °C. Analysis was carried out under gradient conditions. Two mobile phases were used for chromatographic separation: solvent A consisted of 2 mM ammonium acetate: methanol (95:5, v/v) and solvent B consisted of 2 mM ammonium acetate:acetonitrile:methanol (5:15:80, v/v/v). The flow rate was 0.3 ml/min. CsA metabolites were eluted under a linear gradient increased from 70 to 100% over 10.4 min, held at 100% until 17.5 min, returned to the initial conditions in 0.5 min, and then maintained for 2 min. AM1, AM1c, AM9 and AM4N were identified by comparing their retention times with those of the authentic standards. The shift in retention times within one batch was less than 2%.

Mass spectrometry was performed on a Micromass Quattro II tandem quadrupole mass spectrometer (Micro-

mass Ltd., Manchester, UK). High-performance liquid chromatography eluate was introduced into a stainless steel capillary sprayer held at 3.5 kV through 50 μm silica tubing with a desolvation temperature of 300 °C. The positive electrospray (ES+) mode was employed. The cone voltage was 45 eV and the collision energy was 60 eV. The precursor ions (MH^+) of CsA and AM4N were detected at *m/z* 1202.7 and 1188.7, respectively. Multiple reaction monitoring (MRM) was used for AM1, AM1c and AM9. The ion transitions were 1218.7 > 224.2 (for AM1 and AM1c) and 1218.7 > 212.1 (for AM9). Data acquisition and analysis were carried out using MassLynx-NT® 3.4 (Micromass Ltd.).

The calibration curves for AM1, AM1c, AM4N and AM9 were generated by plotting the peak area of these metabolites against their concentrations (1–200 ng/ml). Each point on the calibration curve was generated in duplicate and six points were used for each standard curve. The detection limit for CsA metabolites was 100 pg/ml. Intra- and inter-day variability for the quantitation of CsA metabolites was less than 10 and 15%, respectively.

2.7. Mass spectrometric identification of AM19 and AM1c9

The same HPLC and mass spectrometry conditions described above were used to separate secondary metabolites of CsA. Precursor ions (MH^+) of di-hydroxylated metabolites were detected at *m/z* 1234.8 in the single ion reaction (SIR) mode. Samples from incubations with heterologously expressed enzymes were also used to scan for the product ions of MH^+ 1234.8 in continuum mode with a cone voltage of 45 eV and a collision energy of 35 eV. AM19 and AM1c9 peaks from the chromatograph were identified by comparing their fragmentation patterns with those of authentic CsA, AM1, AM1c and AM9 standards.

2.8. Data analysis

Simple hyperbolic (Eq. (1)), sigmoidal and substrate inhibition (Eq. (2)) models were fit to the kinetic data sets using WinNonLin, Version 3.2 (Pharsight Co., Mountain View, CA), with proper weighting schemes. Goodness of fit was evaluated by the *F*-test (for nested models), normal distribution of residuals, coefficient of variation (CV) and the visual inspection of the Michaelis-Menten plots.

$$V = \frac{V_{max}[S]}{(K_m + [S])} \quad (1)$$

$$V = \frac{V_{max}[S]}{(K_m + [S] + [S]^2/K_s)} \quad (2)$$

Statistical analysis was performed by NCSS 2001 (NCSS, Kaysville, UT). The Wilcoxon rank-sum test was used for the comparison of AM9 formation and testosterone 6β-hydroxylation by *CYP3A5*3/*3* and **1/*3* kidney microsomes. A 2-sided unpaired *t*-test was used for the comparison of CsA metabolite formation by *CYP3A5*1*-positive and -negative livers. Normality of the data was confirmed before statistical analysis. *P* values less than 0.05 were considered statistically significant.

3. Results

3.1. Cyclosporine A metabolic profiles and kinetics from heterologously expressed CYP3A4 and CYP3A5

When cyclosporine A (0–256 μM) was incubated with CYP3A4 and CYP3A4 + b_5, three major metabolites (AM1, AM9 and AM4N) were detected (Fig. 1). The formation of AM1 and AM9 was NADPH-dependent. The formation of AM4N was also NADPH-dependent. However, at higher CsA concentrations, there was a non-enzyme generated appearance of a signal in the AM4N channel (*m/z* 1188.7). AM1c was not detected under these incubation conditions.

The metabolism of CsA by CYP3A4 showed substrate inhibition kinetics for the formation of AM1 and AM9 (Fig. 2a). A substrate inhibition model provided the best fit of the data. Kinetic parameter estimates (Table 1) indicated a relatively high affinity (K_m ~2 μM) for binding that led to product formation and low affinity binding (K_s ~400–500 μM) that reduced the reaction rate. We also tested whether co-expression of cytochrome b_5 with CYP3A4 and P450 reductase would alter the reaction kinetics. As seen in Table 1, the formation of AM1 and AM9 by CYP3A4 + b_5 also exhibited substrate inhibition kinetics, although the estimated V_{max} for both reactions was 2–2.5 times greater than that observed when exogenous cytochrome b_5 was added to the CYP3A4 preparation. In contrast, both K_m and K_s for the different CYP3A4 preparations were similar.

Incubation of CsA (0–256 μM) with CYP3A5 yielded only one primary metabolite—AM9. Other metabolites were not detected under these experimental conditions. The formation of AM9 by CYP3A5 again displayed substrate inhibition kinetics (Fig. 2b) and model fitting (Eq. (2)) yielded a higher K_s (seven-fold) and V_{max} (nine-fold) than the comparable b_5-supplemented CYP3A4 preparation (Table 1).

3.2. Western blot analysis of kidney microsomes

Of the 20 human kidneys selected for analysis, four exhibited a *CYP3A5*1/*3* genotype [35]. The other 16 kidneys all had a *CYP3A5*3/*3* genotype. A representative Western blot of kidney microsomes probed with a selective CYP3A5 antibody is shown in Fig. 3. Only one band was detected and it co-migrated with authentic CYP3A5

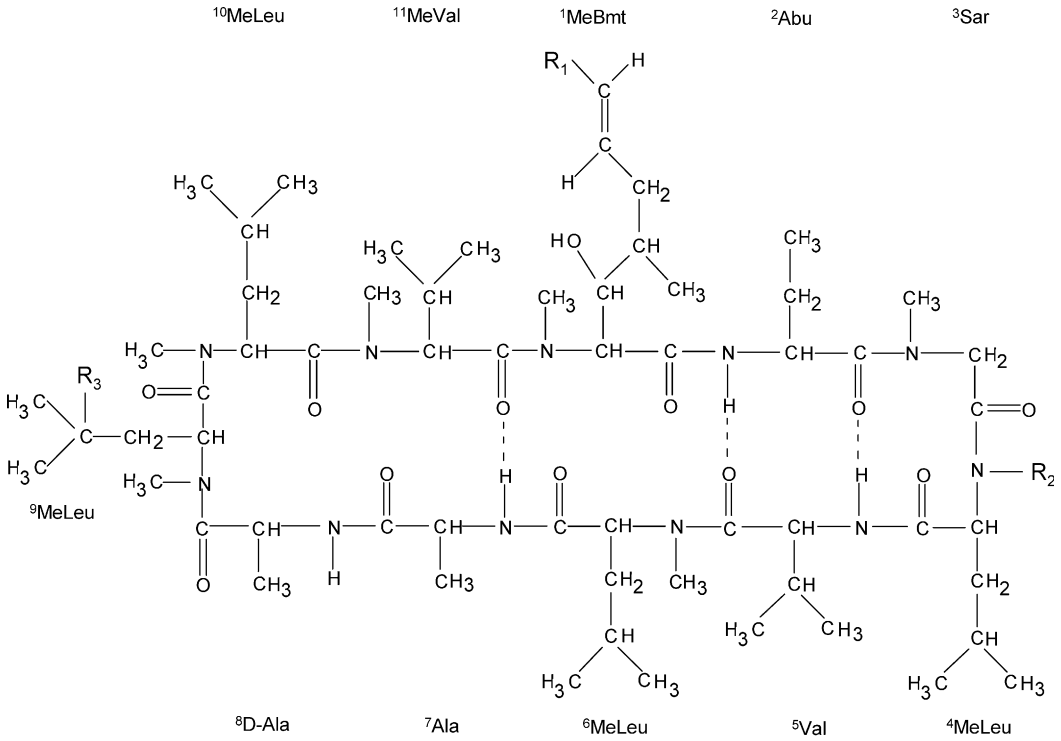

Metabolite	R_1	R_2	R_3
CsA	CH_3	CH_3	H
AM1	CH_2OH	CH_3	H
AM1c	CH_2OH (^{1}MeBmt: cyclization)	CH_3	H
AM4N	CH_3	H	H
AM9	CH_3	CH_3	OH
AM19	CH_2OH	CH_3	OH
AM1c9	CH_2OH (^{1}MeBmt: cyclization)	CH_3	OH

Fig. 1. Structure of cyclosporine A ($C_{62}H_{111}N_{11}O_{12}$) and its major metabolites.

standard. The average CYP3A5 content was eight-fold higher in **1/*3* kidneys than that of **3/*3* kidneys. No CYP3A4 was detected in any of the kidney microsomal preparations (data not shown). Microsomal preparations from four *CYP3A5*1/*3* and four *CYP3A5*3/*3* kidneys were used for further experimentation.

3.3. Renal microsomal testosterone 6β-hydroxylation activity

Testosterone 6β-hydroxylation activity for the different renal microsomal preparations was measured to confirm that the CYP3A5 detected by Western blot analysis was catalytically competent. Although there was significant inter-individual variability, formation of 6β-hydroxytestosterone was on average seven-fold higher for *CYP3A5*1/*3* microsomes ($P = 0.03$), compared to microsomes from *CYP3A5*3/*3* kidneys (Fig. 4a).

3.4. Cyclosporine A metabolic profiles and kinetics from human kidney microsomes

When CsA was incubated with kidney microsomes, AM9 was the only metabolite detected. The rates of AM9 formation were 30- and 17-fold higher for *CYP3A5*1/*3* microsomes than *CYP3A5*3/*3* microsomes at CsA concentrations of 2 μM ($P = 0.04$) and 20 μM ($P = 0.03$), respectively (Fig. 4b and c).

CsA (2–45 μM) was incubated with one of the *CYP3A5*1/*3* microsomal preparations (HK-114B) which had the highest activity for AM9 formation. The simple hyperbolic model provided the best fit to the data (Fig. 5), yielding a K_m that was similar to that obtained from heterologously expressed CYP3A5 (Table 1). There was no evidence of substrate inhibition (unlike CYP3A5), but a more robust substrate concentration range that might have revealed the phenomenon could not be explored because of

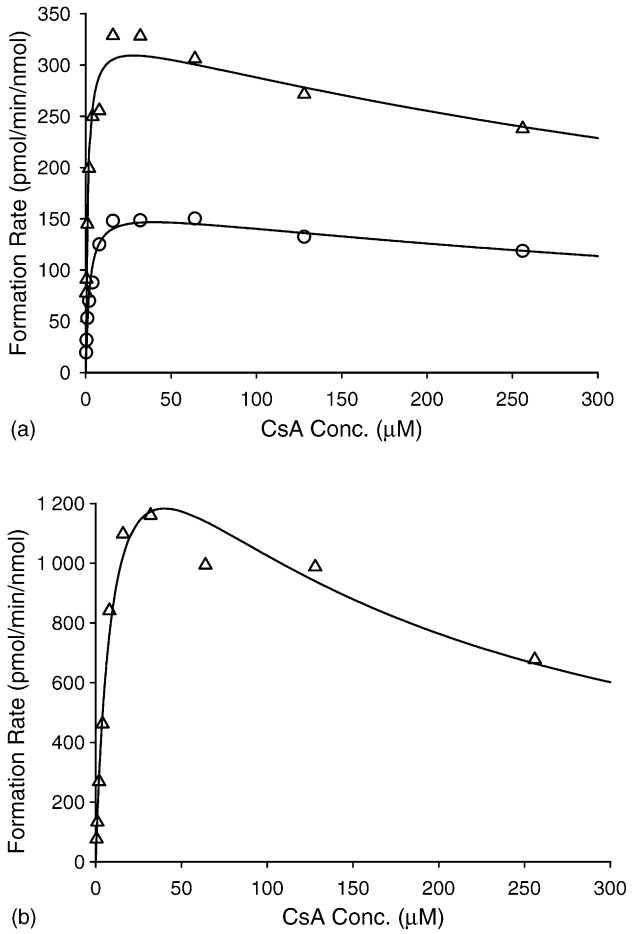

Fig. 2. Model fits for the formation of AM1 (circle) and AM9 (triangle) by CYP3A4 (a) or CYP3A5 (b) supplemented (1:3 molar ratio) with cytochrome b_5.

enzyme limitations. Co-incubation with the CYP3A selective inhibitor ketoconazole (200 nM) caused a 22–55% reduction of AM9 formation over a CsA concentration range of 2–45 μM.

3.5. Cyclosporine A metabolic profiles of microsomes from human livers with CYP3A5*1/*3 and *3/*3 genotypes

Incubation of CsA with liver microsomes yielded three major metabolites AM1, AM9 and AM4N. The rate of AM1 formation was slightly higher (41–54%, not significant), on average, for *CYP3A5*1/*3* liver microsomes compared to **3/*3* liver microsomes at the two different CsA concentrations tested (Table 2). However, the rate of AM9 formation was, on average, greater than two-fold higher for liver microsomes with a *CYP3A5*1/*3* genotype than those with a **3/*3* genotype at 2 μM CsA ($P = 0.013$) and 20 μM CsA ($P = 0.001$), respectively (Table 2). AM4N was only detected in incubations with 20 μM CsA. The mean rate of AM4N formation from *CYP3A5*1/*3* microsomes was approximately twice that of *CYP3A5*3/*3* livers, but the difference was not significant.

3.6. Formation and mass spectrometric analysis of AM19 and AM1c9 in kidney and liver microsomes with CYP3A5*1/*3 and *3/*3 genotypes

To generate the secondary metabolites of CsA, parent drug, AM1 and AM1c were incubated with CYP3A4 and CYP3A5. Two peaks with retention times of 11.8 (P11.8) and 12.3 (P12.3) min were identified on SIR chromatograms for *m/z* 1234.8 (mass consistent with dihydroxylation of CsA) (data not shown). AM19 and AM1c9 eluted earlier than the mono-hydroxylated metabolites AM1, AM9 and AM1c (retention time: 13.6, 13.8 and 14.1 min, respectively), which was consistent with the fact that di-hydroxylated metabolites are more hydrophilic. Due to a lack of authentic standards, P11.8 and P12.3 from CYP3A4 and CYP3A5 incubations were then subjected to MS–MS analysis by scanning in a continuous mode for the product ions of *m/z* 1234.8 and comparing the fragmentation pattern with those of CsA and its primary

Table 1
Kinetic parameters for CsA metabolite formation by heterologous baculovirus-insect cell expressed CYP3A4, CYP3A4 + b_5 and CYP3A5, and *CYP3A5*1/*3* kidney microsomes

CsA metabolites	V_{max} (pmol/min/nmol)	K_m	CI_{int} (μl/min/nmol)	K_s (μM)
CYP3A4				
AM1	141 ± 51	2.2 ± 0.2	66 ± 30	500 ± 177
AM9	288 ± 57	1.6 ± 0.8	214 ± 110	401 ± 214
AM1 + AM9			281 ± 138	
CYP3A4 + b_5				
AM1	304 ± 66	1.3 ± 0.4	237 ± 18	455 ± 206
AM9	757 ± 188	1.2 ± 0.4	684 ± 233	380 ± 124
AM1 + AM9			921 ± 248	
CYP3A5				
AM9	1330 ± 411	11.3 ± 2.6	122 ± 46	166 ± 33
HK-114B				
AM9	71.2	15.5	4.6	

CYP3A4 and CYP3A5 were supplemented (1:3 molar ratio) with cytochrome b_5. Each parameter estimate (mean ± S.D.) was determined from three different experiments.

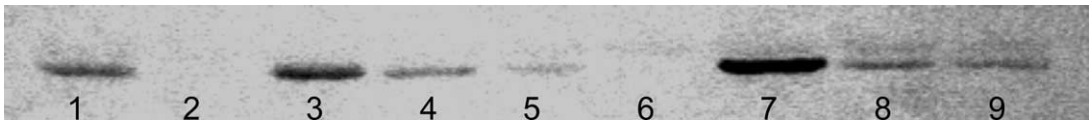

Fig. 3. Western blot of human kidney microsomes probed with anti-CYP3A5 IgG. The analysis was performed as described in Section 2. Lanes 1, 2, and 6–9 contained 50 μg microsomal protein from kidneys with a *CYP3A5*1/*3* (lanes 1, 7, 8, 9) or *CYP3A5*3/*3* (lanes 2, 6) genotype. Lanes 3–5 contained 0.5, 0.25, and 0.125 pmol CYP3A5 standard, respectively.

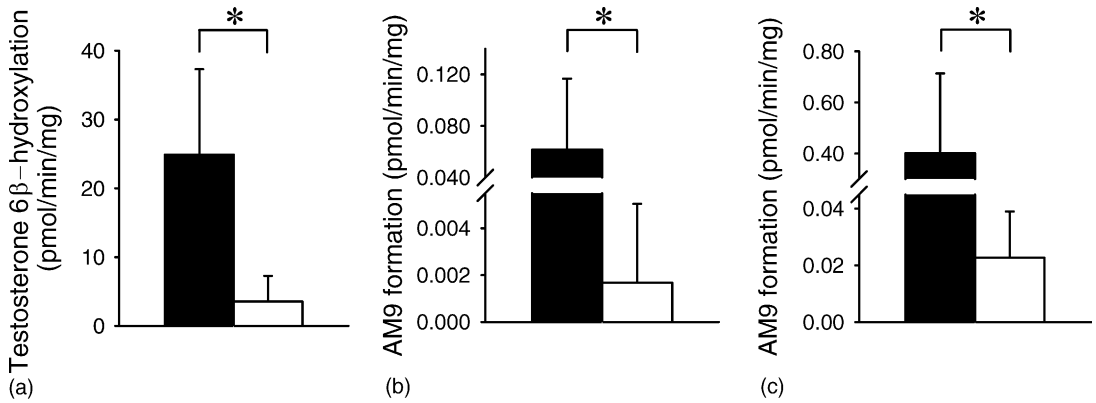

Fig. 4. Effect of *CYP3A5* genotype on renal microsomal catalytic activity. Microsomes from tissues with a *CYP3A5*1/*3* (filled bar) and *CYP3A5*3/*3* (empty bar) genotype were incubated with testosterone (200 μM) (a) or CsA (2 or 20 μM) (b and c), as described in Section 2. Mean rates of 6β-hydroxytestosterone and AM9 formation for the different genotype groups were compared by application of a Wilcoxon rank-sum test. A significant difference ($P < 0.05$) is denoted with an asterisk.

metabolites (Table 3). The fragmentation patterns of P11.8 and P12.3 further revealed their identity. An increment of 16 mass unit was seen in the product ions containing amino acid ^{1}MeBmt (212.1 → 228.1) and ^{9}MeLeu (524.4 → 540.4, 637.5 → 653.5 and 934.7 → 950.7) but not in those containing other amino acids (425.3 and 567.4). Interestingly, the *m/z* 678.5 fragment was only seen for AM1c and AM1c9 but not for other metabolites. This ion could arise from a fragment including MeBmt (with cyclization). However, product ions of this fragment revealed that it could also be generated from different parts of the molecule (data not shown). Fragments *m/z* 1089.8 and 1105.7 (corresponding to the loss of the side chain of ^{1}MeBmt), which have been used previously to identify CsA metabolites, were not very obvious. This could be due to instrument differences as well as fragmentation conditions. Also, as pointed out by Havlicek et al. [47], these fragments could arise from the loss of other parts of the

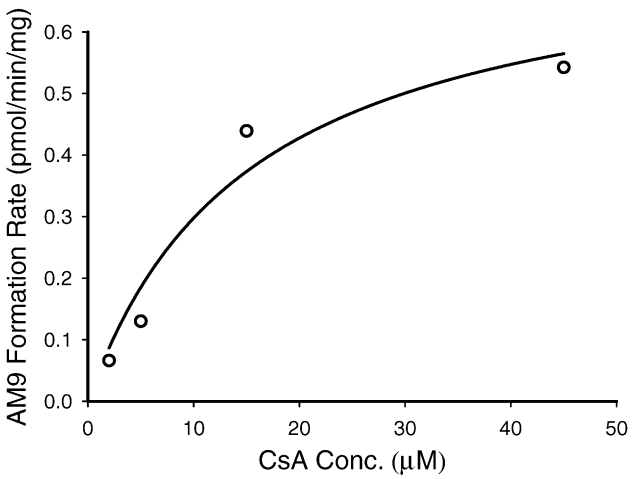

Fig. 5. Michaelis-Menten plot of AM9 formation by kidney microsome HK-114B. A simple hyperbolic model (Eq. (1)) was fit to the data; K_m = 15.5 μM, V_{max} = 71.2 pmol/min/nmol CYP3A5.

Table 2
Formation rates of CsA primary metabolites by *CYP3A5*3/*3* and **1/*3* liver microsomes incubation with 2 μM and 20 μM CsA

CsA metabolites (pmol/min/mg protein)	2 μM CsA		20 μM CsA	
	*CYP3A5*3/*3*	*CYP3A5*1/*3*	*CYP3A5*3/*3*	*CYP3A5*1/*3*
AM1	5.6 ± 3.4 (2.26–11.92)	8.6 ± 3.6 (3.0–14.1)	10.8 ± 6.3 (2.7–24.7)	15.1 ± 8.0 (4.6–29.3)
AM9	22.7 ± 15.1 (8.8–51.4)	50.5 ± 28.2* (13.7–104)	34.0 ± 18.9 (8.0–68.5)	103 ± 52** (43–193)
AM4N	ND	ND	2.4 ± 2.3 (0–5.8)	4.7 ± 4.3 (0–14.5)

Each value represents mean ± S.D. with lowest and highest values in the parenthesis. ND = not determined.
* $P = 0.01$ compared with *CYP3A5*3/*3* microsomes.
** $P = 0.001$ compared with *CYP3A5*3/*3* microsomes

Table 3
Fragmentation patterns of P11.8 and P12.3 and comparison with those of CsA, AM1, AM1c and AM9

Fragment structure	Mass calculated [M + H]	Mass measured [M + H]					
		CsA	AM1	AM1c	AM9	P11.8	P12.3
^{1}MeBmt + C=O	212.1	212.1 (4.84)	–	–	212.2 (35.36)	212.5 (0.05)	212.3 (0.02)
^{1}MeBmt + C=O + [O]	228.1	–	228.2 (6.72)	228.2 (17.48)	–	228.2 (11.12)	228.3 (29.61)
Undetermined	224.1	224.2 (6.20)	224.3 (21.35)	224.3 (12.56)	224.1 (0.11)	224.3 (0.21)	224.3 (0.11)
^{6}Val-^{7}Ala-^{8}D-Ala-^{9}MeLeu	397.3	397.2 (2.92)	397.4 (10.59)	397.4 (6.86)	397.2 (0.03)	397.3 (0.22)	397.3 (0.13)
^{6}Val-^{7}Ala-^{8}D-Ala-^{9}MeLeu + [O]	413.3	–	–	413.3 (0.10)	413.4 (1.71)	413.5 (1.63)	413.3 (0.85)
^{3}Sar-^{4}MeLeu-^{5}Val-^{6}MeLeu	425.3	425.3 (5.78)	425.4 (14.13)	425.4 (11.23)	425.4 (7.97)	425.5 (4.65)	425.4 (4.36)
^{3}Sar-^{4}MeLeu-^{5}Val-^{6}MeLeu + [O]	441.3	–	–	–	–	441.6 (0.35)	441.5 (0.48)
^{6}Val-^{7}Ala-^{8}D-Ala-^{9}MeLeu-^{10}MeLeu	524.4	524.4 (1.52)	524.5 (8.46)	524.6 (3.59)	524.6 (0.02)	–	524.4 (0.01)
^{6}Val-^{7}Ala-^{8}D-Ala-^{9}MeLeu-^{10}MeLeu + [O]	540.4	–	540.4 (0.02)	540.5 (0.03)	540.4 (1.17)	540.5 (0.83)	540.6 (0.64)
^{3}Sar-^{4}MeLeu-^{5}Val-^{6}MeLeu-^{7}Ala-^{8}D-Ala	567.4	567.4 (0.96)	567.5 (1.47)	567.6 (1.38)	567.4 (0.33)	567.5 (0.48)	567.5 (0.32)
^{3}Sar-^{4}MeLeu-^{5}Val-^{6}MeLeu-^{7}Ala-^{8}D-Ala + [O]	583.4	–	583.3 (0.01)	583.4 (0.05)	583.5 (0.01)	583.3 (0.01)	583.2 (0.07)
^{6}Val-^{7}Ala-^{8}D-Ala-^{9}MeLeu-^{10}MeLeu-^{11}MeVal	637.5	637.6 (2.65)	637.6 (11.25)	637.6 (4.49)	637.5 (0.02)	637.7 (0.01)	637.7 (0.06)
^{6}Val-^{7}Ala-^{8}D-Ala-^{9}MeLeu-^{10}MeLeu-^{11}MeVal + [O]	653.5	–	653.7 (0.05)	653.7 (0.01)	653.6 (0.61)	653.6 (2.83)	653.6 (1.00)
Undetermined	678.5	–	678.5 (0.18)	678.5 (2.37)	678.6 (0.16)	678.4 (0.12)	678.5 (0.69)
^{3}Sar-^{4}MeLeu-^{5}Val-^{6}MeLeu-^{7}Ala-^{8}D-Ala-^{9}MeLeu-^{10}MeLeu-^{11}MeVal	934.7	934.7 (1.51)	934.9 (2.42)	934.8 (1.71)	934.8 (0.33)	–	934.5 (0.02)
^{3}Sar-^{4}MeLeu-^{5}Val-^{6}MeLeu-^{7}Ala-^{8}D-Ala-^{9}MeLeu-^{10}MeLeu-^{11}MeVal + [O]	950.7	–	950.8 (0.14)	–	950.8 (0.39)	950.7 (0.61)	950.7 (0.50)
[M + H] − $C_7H_{13}O_2$ (from ^{1}MeBmt) for CsA [M + H] − $C_7H_{13}O_3$ (from ^{1}MeBmt) for AM1, AM1c	1089.8	–	1089.9 (0.20)	1089.8 (0.26)	1090.0 (0.40)	1089.9 (0.60)	1089.8 (1.05)
[M + H] − $C_7H_{13}O_2$ (from ^{1}MeBmt) for AM9	1105.7	–	1105.9 (2.90)	1105.9 (3.17)	1105.9 (1.26)	1105.9 (0.08)	1105.5 (0.02)

Numbers in parentheses are relative abundance of the fragment.

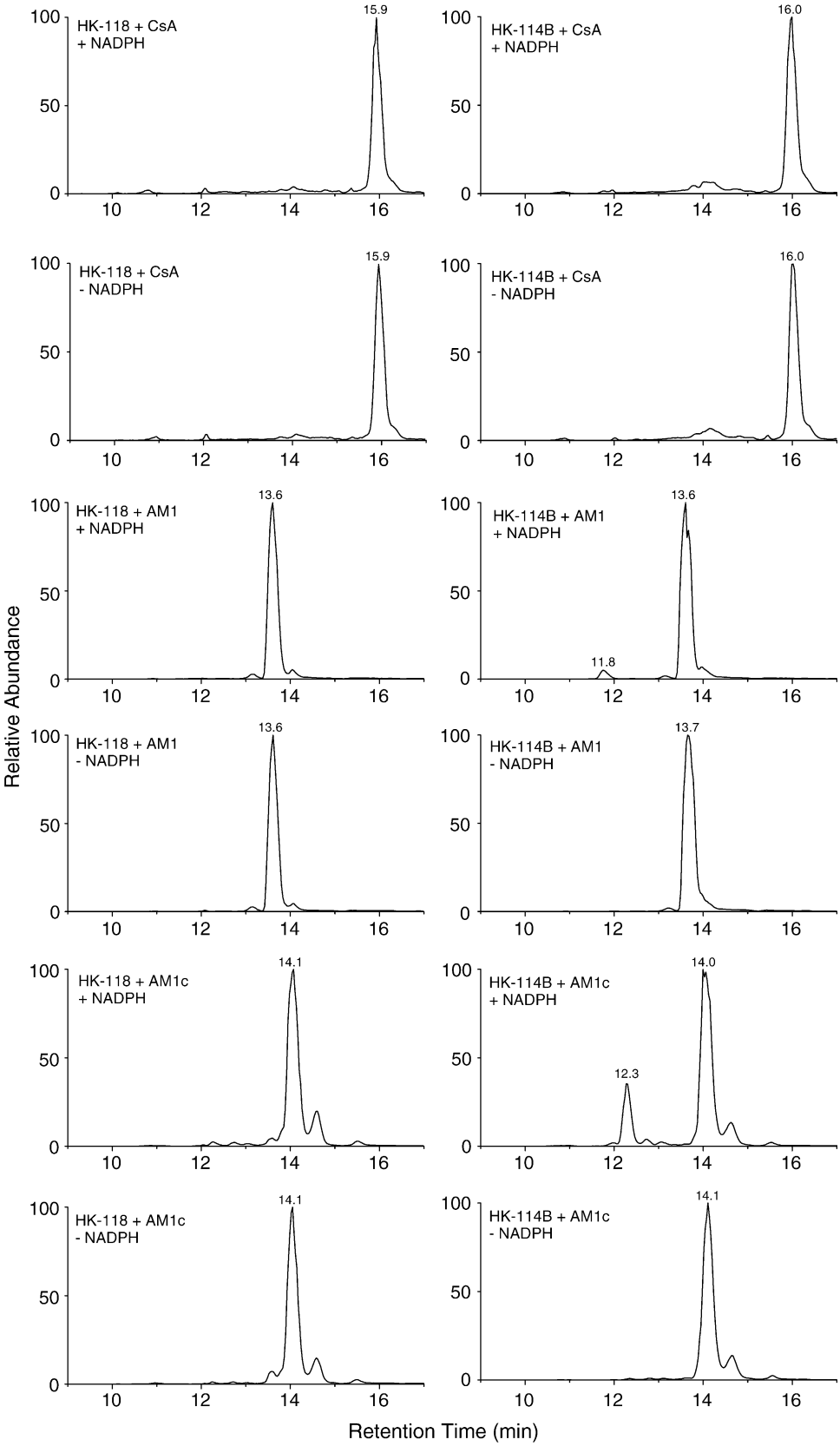

Fig. 6. Chromatograms of SIR of *m/z* 1234.8 for incubation of CsA, AM1 and AM1c (20 μM each) with human kidney microsomes HK-118 (*CYP3A5*3/*3*) and HK-114B (*CYP3A5*1/*3*) for 2 h. Peaks at 11.8 and 12.3 min represent AM19 and AM1c9, respectively. Peaks at 16.0, 13.7 and 14.1 min represent ion overlap from excess CsA, AM1 and AM1c, respectively.

molecules. Based on the aggregate of chromatographic and mass spectrometric results, the detected peaks (P11.8 and P12.3) were identified as AM19 and AM1c9, respectively.

Kidney and liver microsomes from *CYP3A5*1/*3* (HK-114B and HL-144) and *CYP3A5*3/*3* tissues (HK-118 and HL-124) were each incubated with CsA, AM1 and AM1c. For the liver, both *CYP3A5* genotypes yielded AM19 product from CsA and AM1 incubation, and AM1c9 from AM1c incubation. In contrast, only microsomes from *CYP3A5*1* kidneys generated a detectable amount of metabolites; AM19 from incubation with AM1 and AM1c9 from incubation with AM1c (Fig. 6). There were no secondary metabolites when kidney microsomes were incubated with CsA. Peaks detected at 16.0, 13.6 and 14.1 min were from the excess amount of CsA, AM1 and AM1c, respectively.

4. Discussion

Using heterologously expressed human CYP enzymes, we were able to confirm the CsA metabolic profiles for CYP3A4 and CYP3A5. CsA was biotransformed by CYP3A4 to the major primary metabolites, AM1, AM9 and AM4N. In contrast, only AM9 was formed by CYP3A5. This was consistent with the findings of Aoyama et al. [20] and illustrates that CYP3A4 and CYP3A5 often exhibit different product regioselectivity toward a common substrate. CYP3A4 oxidizes CsA at multiple positions (^{1}MeBmt, ^{4}MeLeu, ^{9}MeLeu, etc.) while CYP3A5 preferentially attacks at amino acid 9 (^{9}MeLeu) (Fig. 1). There are other examples of CYP3A5 substrates for which there is a marked difference in the product regioselectivity, compared to CYP3A4, including mifepristone [48], midazolam [49], tacrolimus [50] and aflatoxin B_1 [43]. Interestingly, AM1c, one of the major metabolites found in vivo, was not detected under the incubation conditions used in this study. This was a clear example where in vitro experiments do not recapitulate the in vivo metabolic profile in every aspect.

Three different heterologously expressed human CYP3A preparations were used to estimate the kinetic parameters (V_{max} and K_m) for the formation of AM1 and AM9. Among them, CYP3A4 and CYP3A5 were co-expressed with NADPH-dependent cytochrome P450 reductase and supplemented with cytochrome b_5 (CYP/b_5 molar ratio = 1:3). The formation of AM1 and AM9 by CYP3A4 and AM9 by CYP3A5 all conformed to substrate inhibition kinetics, a phenomenon commonly encountered in CYP3A catalyzed reactions [51]. However, CYP3A5 showed a 5- to 10-fold higher K_m for the formation of AM9 but also a higher V_{max}. The net effects were a comparable or slightly lower intrinsic clearance for the formation of AM9 by CYP3A5 than CYP3A4, indicating a potential role for CYP3A5 in the metabolic clearance of CsA. This interpretation could be biased somewhat by the unequal level of P450 reductase activity in the CYP3A4 and CYP3A5 preparations. It could also be skewed by the unnatural mechanism of introducing cytochrome b_5 into the catalytic system, as evidenced by the two- to three-fold higher k_{cat} for CYP3A4 when it was co-expressed with b_5. However, results from hepatic microsomal incubations suggest that any methodological artifacts of CYP3A comparison were minor and argue in favor of a significant role for CYP3A5 in the production of AM9 and CsA elimination.

It was noted that the rates of formation of AM1 and AM4N, metabolites not seen in CYP3A5 incubations, were 50–90% higher for *CYP3A5*1/*3* than for *CYP3A5*3/*3* liver microsomes. Although the differences were not statistically significant, they suggested the possibility that although the two groups of liver microsomes had matched immunodetectable CYP3A4 contents they were not equally matched with respect to specific CYP3A4 activity (possibly due to different percentages of apo- and holoenzyme). We recently found that itraconazole hydroxylation is readily catalyzed by CYP3A4, but not at all by CYP3A5 [52]. Adjustment of the hepatic microsomal AM1 and AM4N activities for the corresponding maximal rate of itraconazole hydroxylation of each microsomal preparation greatly diminished the absolute and relative differences in AM1 and AM4N formation. In contrast, the adjusted AM9 formation rate remained significantly higher for *CYP3A5*1/*3*, compared with *CYP3A5*3/*3* microsomes (data not shown).

Because the AM9 pathway is only one of three primary elimination routes, the total metabolic clearance in vivo should be only modestly affected by the *CYP3A5* genotype. This prediction is consistent with in vivo observations. In a recent publication [53], Haufroid et al. reported significantly higher (1.6-fold) dose-adjusted trough CsA concentrations in kidney transplant patients with a *CYP3A5*3/*3* genotype, compared to *CYP3A5*1/*3* heterozygotes. In contrast, Hesselink et al. [54] found that CsA trough blood level following an oral dose was poorly associated with the *CYP3A5* polymorphism in kidney transplant patients. However, the authors argued that this lack of association could be due to the poor correlation of the CsA trough blood level with CsA AUC. An alternative explanation is that CYP3A4 is the dominant isoform for CsA clearance in vivo and that uncontrolled variability in this parameter can mask the penetrance of the *CYP3A5* polymorphism, particularly in studies of limited sample size.

Although these findings suggest a limited effect of the *CYP3A5* polymorphism on total oral CsA clearance in vivo, the product regioselectivity of CYP3A5 could result in more profoundly altered metabolite patterns in blood and, more interestingly, in the kidney epithelial cells. Only CYP3A5 (and not CYP3A4) was expressed in human kidneys, a finding consistent with published works from other research groups [33,34]. However, CYP3A5 is a

polymorphic enzyme. Western blot analysis demonstrated that CYP3A5 was only detected in the four *CYP3A5*1/*3* kidney microsomes, and not in *CYP3A5*3/*3* microsomes. Moreover, significant AM9 formation was only detected in incubations from a *CYP3A5*1/*3* donor. Although a trace amount of AM1 and AM4N were also detected in the kidney microsomal incubation, it was more likely due to non-specific formation (also seen without adding NADPH) than CYP3A5 activity. The selectivity of renal CYP3A5 for AM9 formation that we report is in contrast with the results of Vickers et al. [55] who found that only AM1 (M17) was formed in human kidney slices and microsomes prepared from four organ donors. However, their rates of AM1 formation from kidney microsomes (0.05 pmol/h/mg) incubated with 1 μM CsA were much less than that of AM9 formation (3.7 pmol/h/mg) from our *CYP3A5*1/*3* microsomes incubated with 2 μM CsA. One plausible explanation for this discrepancy could be that the four organ donors from the previous study were all *CYP3A5*3/*3* and that low levels of AM1 could be formed by other enzymes.

Kinetic data for AM9 formation from the *CYP3A5*1/*3* microsomes provided additional evidence that only CYP3A5 contributed significantly to CsA metabolism in the human kidney (Table 1). The K_m for the renal-catalyzed reaction (15.5 μM) was similar to that obtained from CYP3A5 (11.3 μM). However, we did note that the specific activity of renal CYP3A5 (nmol product/min/nmol CYP3A5) was 20-fold lower than that observed for expressed CYP3A5 (Table 1). This could be due to a loss of CYP3A5 activity, but not protein, in these kidney samples during the long procurement period before cryopreservation, since these kidneys were the organs rejected for transplantation nation-wide. It could also reflect suboptimal P450 reductase and cytochrome b_5 activity.

The positive association between high testosterone 6β-hydroxylation and AM9 formation and *CYP3A5*1* genotype also supports the conclusion of a major role for CYP3A5 in renal AM9 formation, as does the observed inhibition from co-incubation of renal microsomes with CsA and ketoconazole (200 nM). Considering the K_i value for ketoconazole and CYP3A5 (109 nM, Gibbs et al. [45]) and the possible effect of non-specific protein binding on the free concentration of ketoconazole [56] in the incubation with 0.4 mg renal microsomal protein, the incomplete 22–55% inhibition of AM9 formation with a nominal 200 nM CsA concentration was not that surprising.

AM19 and AM1c9 were formed by both *CYP3A5*1/*3* and *CYP3A5*3/*3* liver microsomes with a much higher specific activity than kidney microsomes (based on a comparison of the ion current). This was not surprising since CYP3A4 was expressed in all of the liver microsomes. Without authentic standard, the rate of AM19 and AM1c9 formation in liver microsomes with different *CYP3A5* genotypes could not be determined. However, it is likely that *CYP3A5*1/*3* liver microsomes would have higher AM19 and AM1c9 formation rates than *CYP3A5*3/*3* liver microsomes, as was the case for AM9 formation. In contrast to the liver, AM19 and AM1c9 were formed from AM1 and AM1c almost exclusively by kidney microsomes with a *CYP3A5*1/*3* genotype, and not by *CYP3A5*3/*3* microsomes (Fig. 6). In addition, only AM9 and a small amount of AM19 was formed from CsA by renal microsomes, since little AM1 was generated in the absence of CYP3A4. Based on these results, one might anticipate higher circulating blood concentrations of AM9, AM19 and AM1c9 in patients carrying the wild-type *CYP3A5*1* allele compared to those homozygous for the mutant allele(s), a difference mediated by intestinal and hepatic metabolism. One might also anticipate higher AM9, AM19 and AM1c9 levels in the kidneys of patients with a *CYP3A5*1* genotype. Circulating CsA, AM1 and AM9 are all substrates for kidney CYP3A5 in *CYP3A5*1/*3* individuals, resulting in the formation of AM9, AM19 and AM1c9, respectively. This organ-specific biotransformation step would not be seen in *CYP3A5*3/*3* individuals.

Elevated blood and urine levels of AM19 and AM1c9 have been associated with renal dysfunction in cyclosporine treated patients [31,32]. This change may simply represent a biomarker of CsA nephrotoxicity, reflecting impaired renal elimination. However, the pharmacokinetic change may also be mechanistically linked to renal toxic events and renal CYP3A5 activity. Although the primary and secondary metabolites of CsA are generally equivalent or less toxic than CsA in cultured renal epithelial cells [27,28], AM19 and AM1c9 (but not CsA or its primary metabolites) have been shown to alter renal mesangial cell function (increased endothelin release) [7]. Thus, increased exposure of renal cells to the secondary CsA metabolites in patients with a *CPY3A5*1* genotype may increase the risk of CsA treatment-related nephrotoxicity. In addressing this hypothesis, it will also be important to consider the function of renal P-glycoprotein and polymorphisms in the *ABCB1* gene that have been associated with the risk of renal toxicity from cyclosporine inhibitor therapy [2]. High P-glycoprotein activity may counteract any negative effects from renal AM19 and AM1c9 formation, if these metabolites are also substrates for active efflux.

Acknowledgements

The authors thank Dr. William N. Howald, Ross F. Lawrence, Thomas F. Kalhorn and Dr. Catalin E. Doneanu for their assistance and advice in mass spectrometric quantification and analysis of cyclosporine metabolites. Financial support for this work was provided in part by grants from the National Institutes of Health; GM63666, GM32165, and P30ES07033.

References

[1] Ojo AO, Held PJ, Port FK, Wolfe RA, Leichtman AB, Young EW, et al. Chronic renal failure after transplantation of a nonrenal organ. N Engl J Med 2003;349(10):931–40.

[2] Hebert MF, Dowling AL, Gierwatowski C, Lin YS, Edwards KL, Davis CL, et al. Association between ABCB1 (multidrug resistance transporter) genotype and post-liver transplantation renal dysfunction in patients receiving calcineurin inhibitors. Pharmacogenetics 2003;13(11):661–74.

[3] Fisher NC, Nightingale PG, Gunson BK, Lipkin GW, Neuberger JM. Chronic renal failure following liver transplantation: a retrospective analysis. Transplantation 1998;66(1):59–66.

[4] Lynn M, Abreo K, Zibari G, McDonald J. End-stage renal disease in liver transplants. Clin Transplant 2001;15(Suppl. 6):66–9.

[5] Gonwa TA, Mai ML, Melton LB, Hays SR, Goldstein RM, Levy MF, et al. End-stage renal disease (ESRD) after orthotopic liver transplantation (OLTX) using calcineurin-based immunotherapy: risk of development and treatment. Transplantation 2002;72(12):1934–9.

[6] Cohen AJ, Stegall MD, Rosen CB, Wiesner RH, Leung N, Kremers WK, et al. Chronic renal dysfunction late after liver transplantation. Liver Transplant 2002;8(10):916–21.

[7] Copeland KR, Yatscoff RW. Comparison of the effects of cyclosporine and its metabolites on the release of prostacyclin and endothelin from mesangial cells. Transplantation 1992;53(3):640–5.

[8] Healy E, Dempsey M, Lally C, Ryan MP. Apoptosis and necrosis: mechanisms of cell death induced by cyclosporine A in a renal proximal tubular cell line. Kidney Int 1998;54(6):1955–66.

[9] Hortelano S, Castilla M, Torres AM, Tejedor A, Bosca L. Potentiation by nitric oxide of cyclosporin A and FK506-induced apoptosis in renal proximal tubule cells. J Am Soc Nephrol 2000;11(12):2315–23.

[10] Mihatsch MJ, Thiel G, Ryffel B. Cyclosporine nephrotoxicity. Adv Nephrol Necker Hosp 1988;17:303–20.

[11] Abrass CK, Berfield AK, Stehman-Breen C, Alpers CE, Davis CL. Unique changes in interstitial extracellular matrix composition are associated with rejection and cyclosporine toxicity in human renal allograft biopsies. Am J Kidney Dis 1999;33(1):11–20.

[12] Feutren G, Miller C. Low predictive value of cyclosporine level for efficacy or renal dysfunction in psoriasis and idiopathic nephrotic syndrome. Transplant Proc 1990;22(3):1299–302.

[13] Bach JF, Feutren G, Noel LH, Hannedouche T, Landais P, Timsit J, et al. Factors predictive of cyclosporine-induced nephrotoxicity: the role of cyclosporine blood levels. Transplant Proc 1990;22(3):1296–8.

[14] Christians U, Sewing KF. Alternative cyclosporine metabolic pathways and toxicity. Clin Biochem 1995;28(6):547–59.

[15] Christians U, Sewing KF. Cyclosporin metabolism in transplant patients. Pharmacol Ther 1993;57(2/3):291–345.

[16] Lensmeyer GL, Wiebe DA, Carlson IH. Deposition of nine metabolites of cyclosporine in human tissues, bile, urine, and whole blood. Transplant Proc 1988;20(2 Suppl. 2):614–22.

[17] Christians U, Strohmeyer S, Kownatzki R, Schiebel HM, Bleck J, Greipel J, et al. Investigations on the metabolic pathways of cyclosporine. I. Excretion of cyclosporine and its metabolites in human bile—isolation of 12 new cyclosporine metabolites. Xenobiotica 1991;21(9):1185–98.

[18] Christians U, Strohmeyer S, Kownatzki R, Schiebel HM, Bleck J, Kohlhaw K, et al. Investigations on the metabolic pathways of cyclosporine. II. Elucidation of the metabolic pathways in vitro by human liver microsomes. Xenobiotica 1991;21(9):1199–210.

[19] Kronbach T, Fischer V, Meyer UA. Cyclosporine metabolism in human liver: identification of a cytochrome P-450III gene family as the major cyclosporine-metabolizing enzyme explains interactions of cyclosporine with other drugs. Clin Pharmacol Ther 1988;43(6):630–5.

[20] Aoyama T, Yamano S, Waxman DJ, Lapenson DP, Meyer UA, Fischer V, et al. Cytochrome P-450 hPCN3, a novel cytochrome P-450 IIIA gene product that is differentially expressed in adult human liver. cDNA and deduced amino acid sequence and distinct specificities of cDNA-expressed hPCN1 and hPCN3 for the metabolism of steroid hormones and cyclosporine. J Biol Chem 1989;264(18):10388–95.

[21] Saeki T, Ueda K, Tanigawara Y, Hori R, Komano T. Human P-glycoprotein transports cyclosporin A and FK506. J Biol Chem 1993;268(9):6077–80.

[22] Gan LS, Moseley MA, Khosla B, Augustijns PF, Bradshaw TP, Hendren RW, et al. CYP3A-like cytochrome P450-mediated metabolism and polarized efflux of cyclosporin A in Caco-2 cells. Drug Metab Dispos 1996;24(3):344–9.

[23] Wacher VJ, Silverman JA, Zhang Y, Benet LZ. Role of P-glycoprotein and cytochrome P4503A in limiting oral absorption of peptides and peptidomimetics. J Pharm Sci 1998;87(11):1322–30.

[24] Lown KS, Mayo RR, Leichtman AB, Hsiao HL, Turgeon DK, Schmiedlin-Ren P, et al. Role of intestinal P-glycoprotein (mdr1) in interpatient variation in the oral bioavailability of cyclosporine. Clin Pharmacol Ther 1997;62(3):248–60.

[25] Hebert MF. Contributions of hepatic and intestinal metabolism and P-glycoprotein to cyclosporine and tacrolimus oral drug delivery. Adv Drug Deliv Rev 1997;27(2/3):201–14.

[26] Kwei GY, Alvaro RF, Chen Q, Jenkins HJ, Hop CE, Keohane CA, et al. Disposition of ivermectin and cyclosporin A in CF-1 mice deficient in mdr1a P-glycoprotein. Drug Metab Dispos 1999;27(5):581–7.

[27] Bowers LD. Studies of cyclosporine and metabolite toxicity in renal and hepatocyte culture systems. Transplant Proc 1990;22(3):1135–6.

[28] Copeland KR, Thliveris JA, Yatscoff RW. Toxicity of cyclosporine metabolites. Ther Drug Monitor 1990;12(6):525–32.

[29] Lemoine A, Azoulay D, Gries JM, Dennison A, Castaing D, Fredj G, et al. Relationship between graft cytochrome P-4503A content and early morbidity after liver transplantation. Transplantation 1993;56(6):1410–4.

[30] Schmidt LE, Rasmussen A, Kirkegaard P, Dalhoff K. Relationship between postoperative erythromycin breath test and early morbidity in liver transplant recipients. Transplantation 2003;76(2):358–63.

[31] Christians U, Kohlhaw K, Budniak J, Bleck JS, Schottmann R, Schlitt HJ, et al. Cyclosporin metabolite pattern in blood and urine of liver graft recipients. I. Association of cyclosporin metabolites with nephrotoxicity. Eur J Clin Pharmacol 1991;41(4):285–90.

[32] Kempkes-Koch M, Fobker M, Erren M, August C, Gerhardt U, Suwelack B, et al. Cyclosporine A metabolite AM19 as a potential biomarker in urine for CSA nephropathy. Transplant Proc 2001;33(3):2167–9.

[33] Schuetz EG, Schuetz JD, Grogan WM, Naray-Fejes-Toth A, Fejes-Toth G, Raucy J, et al. Expression of cytochrome P4503A in amphibian, rat, and human kidney. Arch Biochem Biophys 1992;294(1):206–14.

[34] Haehner BD, Gorski JC, Vandenbranden M, Wrighton SA, Janardan SK, Watkins PB, et al. Bimodal distribution of renal cytochrome P4503A activity in humans. Mol Pharmacol 1996;50(1):52–9.

[35] Givens RC, Lin YS, Dowling AL, Thummel KE, Lamba JK, Schuetz EG, et al. CYP3A5 genotype predicts renal CYP3A activity and blood pressure in healthy adults. J Appl Physiol 2003;95(3):1297–300.

[36] Kuehl P, Zhang J, Lin Y, Lamba J, Assem M, Schuetz J, et al. Sequence diversity in CYP3A promoters and characterization of the genetic basis of polymorphic CYP3A5 expression. Nat Genet 2001;27(4):383–91.

[37] Hustert E, Haberl M, Burk O, Wolbold R, He YQ, Klein K, et al. The genetic determinants of the CYP3A5 polymorphism. Pharmacogenetics 2001;11(9):773–9.

[38] Lin YS, Dowling AL, Quigley SD, Farin FM, Zhang J, Lamba J, et al. Co-regulation of CYP3A4 and CYP3A5 and contribution to hepatic and intestinal midazolam metabolism. Mol Pharmacol 2002;62(1):162–72.

[39] Paine MF, Khalighi M, Fisher JM, Shen DD, Kunze KL, Marsh CL, et al. Characterization of interintestinal and intraintestinal variations in human CYP3A-dependent metabolism. J Pharmacol Exp Ther 1997;283(3):1552–62.
[40] Lowry OH, Rosebrough NJ, Farr AL, Randall RJ. Protein measurement with the Folin phenol reagent. J Biol Chem 1951;193:265–75.
[41] Omura T, Sato R. The carbon monoxide-binding pigment of liver microsomes. J Biol Chem 1964;239:2370–85.
[42] Thummel KE, Shen DD, Podoll TD, Kunze KL, Trager WF, Hartwell PS, et al. Use of midazolam as a human cytochrome P4503A probe. I. In vitro–in vivo correlations in liver transplant patients. J Pharmacol Exp Ther 1994;271(1):549–56.
[43] Gillam EM, Guo Z, Ueng YF, Yamazaki H, Cock I, Reilly PE, et al. Expression of cytochrome P4503A5 in *Escherichia coli*: effects of 5′ modification, purification, spectral characterization, reconstitution conditions, and catalytic activities. Arch Biochem Biophys 1995;317(2):374–84.
[44] Fisher MB, Thompson SJ, Ribeiro V, Lechner MC, Rettie AE. P450-catalyzed in-chain desaturation of valproic acid: isoform selectivity and mechanism of formation of Delta 3-valproic acid generated by baculovirus-expressed CYP3A1. Arch Biochem Biophys 1998;356(1):63–70.
[45] Gibbs MA, Thummel KE, Shen DD, Kunze KL. Inhibition of cytochrome P-4503A (CYP3A) in human intestinal and liver microsomes: comparison of K_i values and impact of CYP3A5 expression. Drug Metab Dispos 1999;27(2):180–7.
[46] Simpson J, Zhang Q, Ozaeta P, Aboleneen H. A specific method for the measurement of cyclosporin A in human whole blood by liquid chromatography-tandem mass spectrometry. Ther Drug Monitor 1998;20(3):294–300.
[47] Havlicek V, Jegorov A, Sedmera P, Ryska M. Sequencing of cyclosporins by fast atom bombardment and linked-scan mass spectrometry. Org Mass Spectrom 1993;28(12):1440–7.
[48] Khan KK, He YQ, Correia MA, Halpert JR. Differential oxidation of mifepristone by cytochromes P4503A4 and 3A5: selective inactivation of P4503A4. Drug Metab Dispos 2002;30(9):985–90.
[49] Gorski JC, Hall SD, Jones DR, VandenBranden M, Wrighton SA. Regioselective biotransformation of midazolam by members of the human cytochrome P4503A (CYP3A) subfamily. Biochem Pharmacol 1994;47(9):1643–53.
[50] Bader A, Hansen T, Kirchner G, Allmeling C, Haverich A, Borlak JT. Primary porcine enterocyte and hepatocyte cultures to study drug oxidation reactions. Br J Pharmacol 2000;129(2):331–42.
[51] Lin Y, Lu P, Tang C, Mei Q, Sandig G, Rodrigues AD, et al. Substrate inhibition kinetics for cytochrome P450-catalyzed reactions. Drug Metab Dispos 2001;29(4 Pt 1):368–74.
[52] Isoherranen N, Kunze KL, Allen KE, Nelson WL, Thummel KE. Role of itraconazole metabolites in CYP3A4 inhibition. Drug Metab Dispos 2004;32(10).
[53] Haufroid V, Mourad M, Van Kerckhove V, Wawrzyniak J, De Meyer M, Eddour D, et al. The effect of CYP3A5 and MDR1 (ABCB1) polymorphisms on cyclosporine and tacrolimus dose requirements and trough blood levels in stable renal transplant patients. Pharmacogenetics 2004;14(3):147–54.
[54] Hesselink DA, van Schaik RH, van der Heiden IP, van der Werf M, Gregoor PJ, Lindemans J, et al. Genetic polymorphisms of the CYP3A4, CYP3A5, and MDR-1 genes and pharmacokinetics of the calcineurin inhibitors cyclosporine and tacrolimus. Clin Pharmacol Ther 2003;74(3):245–54.
[55] Vickers AE, Fischer V, Connors S, Fisher RL, Baldeck JP, Maurer G, et al. Cyclosporin A metabolism in human liver, kidney, and intestine slices. Comparison to rat and dog slices and human cell lines. Drug Metab Dispos 1992;20(6):802–9.
[56] Gibbs MA, Kunze KL, Howald WN, Thummel KE. Effect of inhibitor depletion on inhibitory potency: tight binding inhibition of CYP3A by clotrimazole. Drug Metab Dispos 1999;27(5):596–9.